coatings

MDPI

Article

Comparison of Single-Layer and Double-Layer Anti-Reflection Coatings Using Laser-Induced Damage Threshold and Photothermal Common-Path Interferometry

Caspar Clark [1,*], Riccardo Bassiri [2,*], Iain W. Martin [3], Ashot Markosyan [2], Peter G. Murray [3], Des Gibson [4], Sheila Rowan [3] and Martin M. Fejer [2]

1 Helia Photonics Ltd., Livingston EH54 7EJ, UK
2 E. L. Ginzton Laboratory, Stanford University, Stanford, CA 94305, USA; ashotm@stanford.edu (A.M.); fejer@stanford.edu (M.M.F.)
3 Scottish Universities Physics Alliance, School of Physics and Astronomy, University of Glasgow, Glasgow G12 8QQ, UK; Iain.Martin@glasgow.ac.uk (I.W.M.); peter.murray@glasgow.ac.uk (P.G.M.); Sheila.Rowan@glasgow.ac.uk (S.R.)
4 Scottish Universities Physics Alliance, Institute of Thin Films, Sensors & Imaging, School of Engineering and Computing, University of the West of Scotland, Paisley PA1 2BE, UK; des.gibson@uws.ac.uk
* Correspondence: Caspar.Clark@helia-photonics.com (C.C.); rbassiri@stanford.edu (R.B.); Tel.: +44-150-641-4800 (C.C.)

Academic Editor: Alessandro Lavacchi
Received: 29 February 2016; Accepted: 4 May 2016; Published: 10 May 2016

Abstract: The dielectric thin-film coating on high-power optical components is often the weakest region and will fail at elevated optical fluences. A comparison of single-layer coatings of ZrO_2, LiF, Ta_2O_5, SiN, and SiO_2 along with anti-reflection (AR) coatings optimized at 1064 nm comprised of ZrO_2 and Ta_2O_5 was made, and the results of photothermal common-path interferometry (PCI) and a laser-induced damage threshold (LIDT) are presented here. The coatings were grown by radio frequency (RF) sputtering, pulsed direct-current (DC) sputtering, ion-assisted electron beam evaporation (IAD), and thermal evaporation. Test regimes for LIDT used pulse durations of 9.6 ns at 100 Hz for 1000-on-1 and 1-on-1 regimes at 1064 nm for single-layer and AR coatings, and 20 ns at 20 Hz for a 200-on-1 regime to compare the $//ZrO_2/SiO_2$ AR coating.

Keywords: laser-induced damage; photothermal common-path interferometry; optical coatings; 1064 nm

1. Introduction

A need for an AR coating for high-power fused-silica Q-switch components centered at 1064 nm with the ability to survive 20 J/cm^2 prompted this small study to determine the material dependence on the absorption by the photothermal common-path interferometry (PCI) method and a laser-induced damage threshold (LIDT). In Phase 1 of the study, single layers *circa* 500 nm were grown and characterized by spectrophotometric transmission, PCI, and where possible, LIDT. Phase 2 incorporated these materials into double-layer anti-reflection (AR) designs, and a comparison is then made between their single-layer values and those of the subsequent double layer. All coatings were grown at Helia Photonics Ltd. on various substrates, including silicon, Borofloat 33, and Spectrosil 2000 glass witness samples, and, in the case of a few designs, on final fused-silica Q-switch components. LIDT measurements were carried out by Lidaris Ltd. (Vilnius, Lithuania) on the witness samples and for the larger components at Quantel Inc. (Bozeman, MT, USA). PCI measurements were measured at the Ginzton Lab at Stanford University, and atomic force microscopy (AFM) was used in conjunction

with an optical Nomarski assessment at the University of Glasgow. Additional optical measurements including ellipsometric and spectrophotometric assessments were carried out at the University of the West of Scotland.

2. Coating Deposition Techniques and Materials

Thin-film coatings were grown using various deposition systems at Helia Photonics, Scotland, mainly built in-house. The deposition techniques used in this trial were an ion-assisted electron beam (ebeam) with thermal evaporation, radio frequency (RF) sputtering, pulsed direct-current (DC) magnetron sputtering, and thermal evaporation only. An AR coating design was used for all samples and coated on both sides of silica-based substrates including Spectrosil 2000, used for PCI absorption and AFM measurement, and Borofloat 33, used for the LIDT measurements. The substrates were ultrasonically cleaned with an identical solvent process prior to coating to ensure minimal surface contamination. A description of the deposition techniques used and their associated parameters is given in Table 1.

Table 1. Deposition techniques and associated parameters: T = substrate temperature; P = chamber pressure.

Pumping	Source Type	Deposition Parameters
Cryogenic Pump	ion-assisted (End Hall 100 eV) reactive electron beam + thermal	T = 100 °C, 1 m source-substrate, start $P = 1 \times 10^{-6}$ mbar, run $P = 2.5 \times 10^{-3}$ mbar
	pulsed DC (82 kHz) reactive sputtering 4″ magnetrons	T = 150 °C, 15 cm source-substrate, start $P = 1 \times 10^{-6}$ mbar, run $P = 6 \times 10^{-3}$ mbar
	RF (13.56 MHz) reactive sputtering 8″ magnetrons	T = 50 °C, 20 cm source-substrate, start $P = 1 \times 10^{-8}$ mbar, run $P = 8 \times 10^{-3}$ mbar
Turbo Molecular Pump	thermal evaporation, non-reactive, Mo boat	T = 200 °C, 35 cm source-substrate, start $P = 5 \times 10^{-6}$ mbar, run $P = 3 \times 10^{-4}$ mbar

Each coating sample had a material composition chosen due to a variety of practical use scenarios, and the target materials and techniques available at the time of deposition. A description of each coating composition and deposition techniques is given in Table 2. The transmission measurements are also given and were made with a Perkin Elmer Lambda 900 spectrophotometer.

Table 2. Coating material compositions and deposition techniques is given, with measured thicknesses for the single-layer (SL) coatings and transmission (T) values for the anti-reflection (AR) coatings.

#	Coating	SL Thickness (±5 nm) AR T * (±0.1%)	Deposition Techniques
1	$//ZrO_2$	510	RF sputter
2	$//ZrO_2$	515	pulsed DC sputter
3	//LiF	525	thermal
4	$//Ta_2O_5$	480	ebeam
5	//SiN	450	pulsed DC sputter
6	$//SiO_2$	575	pulsed DC sputter
7	$//SiO_2$	590	thermal
8	$//ZrO_2/SiO_2$	99.4	RF sputter
9	$//Ta_2O_5/SiO_2$	99.6	RF sputter
10	$//Ta_2O_5/SiO_2$	99.9	ebeam/thermal
11	$//AlN/SiO_2$	98.6	pulsed DC sputter
12	//AlN/SiN	98.6	pulsed DC sputter
13	$//ZrO_2$/SiN	99.5	pulsed DC sputter
14	//ZnSe/LiF	100.0	thermal

* Transmission by spectrophotometry at 1064 nm on Spectrosil 2000; thickness resolved by transmission spectra.

3. PCI Optical Absorption Measurements

The PCI measurement technique was used to measure the optical absorption of the coatings and is based on measuring the thermal lensing caused by the pump beam (CW, λ = 1064 nm, up to 8 W, spot size = 65 μm) and the resulting interference from the phase mismatch between the central and outermost part of the probe beam (CW, λ = 632 nm, 2.5 mW, spot size = 110 μm). The pump and probe beams cross in the same plane at an angle of 9°, providing an interaction length of 3 mm.

A schematic of the PCI experimental setup is shown in Figure 1. The detected AC voltage (V_{AC}) signal is comprised of only first-order terms and hence can be normalized to the total probe power (DC output voltage (V_{DC}) of the detector) over that of the independent pump power (W_{pump}). Thus, the value of the absorption loss, α, is simply proportional to the ratio $V_{AC}/V_{DC}/W_{pump}$. The setup was calibrated using a Newport metallic neutral density filter, which had an absorption of 22% at 1064 nm (measured with a Cary 500 spectrophotometer). With these parameters, an optical absorption at 1064 nm of α = 0.02 ppm can be measured using pump powers up to 8.0 W. Further details of the measurement setup and process can be found in [1–3].

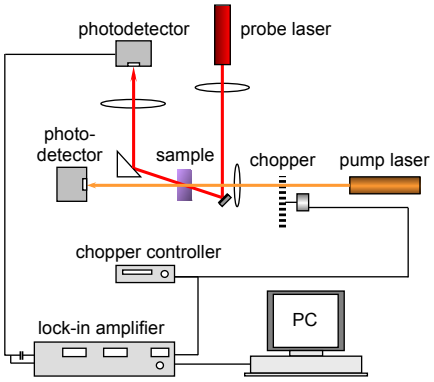

Figure 1. Schematic of the photothermal common-path interferometry (PCI) experimental setup.

The recorded signal is read from the crossing point of the pump and probe beams that move along the pump propagation direction, *i.e.*, perpendicular to the coating in the z-direction (z-scan) or across the coating in the x-direction (x-scan).

In order to ensure the absorption of the coatings is easily distinguishable from the substrate, it is preferable to have a substrate with low absorption compared to the applied coating. The absorption of a sample of Borofloat 33 and Spectrosil 2000 was studied as candidate substrate materials. The Borofloat 33 gave an average α = 2200 ppm/cm with an uneven spread of the PCI signal. The Spectrosil 2000 was chosen as the substrate for the subsequent PCI absorption measurements on the coating samples, as it gave a relatively low and uniform α = 19.5 ppm/cm, as shown in Figure 2.

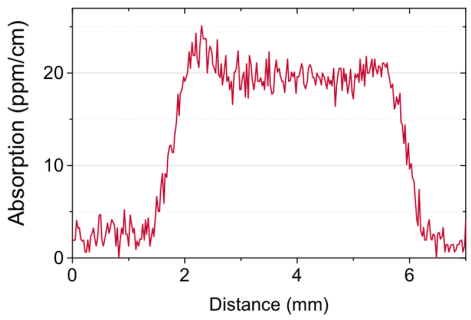

Figure 2. PCI absorption z-scan of the Spectrosil 2000 substrate, with the front surface at 1.8 mm and back surface at 6.0 mm.

PCI x-scans highlighting the best and worst coating absorption values for the ZrO_2 and LiF coating samples are shown in Figure 3. The x-scans probe the absorption across a 6-mm line on the coating. Figure 3a shows the absorption of the single-layer ZrO_2 sample, with a baseline α = 168 ppm, which was the highest single-layer absorption measured. The best single-layer absorption was from the LiF coating (x-scan shown in Figure 3b) with a baseline α = 1 ppm. Spikes in the data may be due to defects such as non-stoichiometric regions, absorbing impurities, and surface contamination; although care is taken to ensure the coating surface is clean and free of any dust during measurement. The baseline PCI absorption values for all of the single-layer coatings studied are given in Table 3, and the absorption is also given in ppm/nm for comparison.

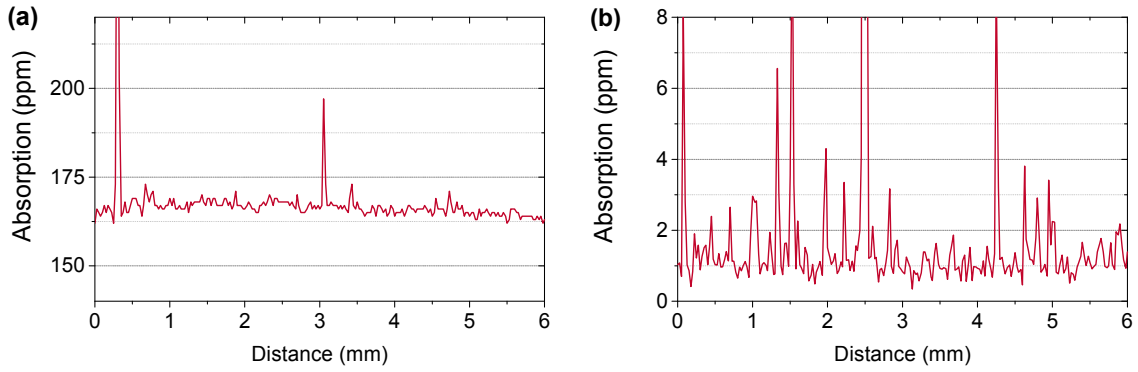

Figure 3. PCI absorption x-scan of the (**a**) DCS ZrO_2; (**b**) thermal LiF single-layer coating samples.

Table 3. PCI baseline absorption values for the single-layer coatings.

Coating and Deposition Technology	PCI Absorption (ppm)	PCI Absorption (ppm/nm)
ZrO_2 RF sputter	79	1.55×10^{-1}
ZrO_2 DC sputter	168	3.26×10^{-1}
LiF thermal	1	1.90×10^{-3}
Ta_2O_5 ebeam	5	1.04×10^{-2}
SiN DC sputter	8	1.78×10^{-2}
SiO_2 DC sputter	1.5	2.61×10^{-3}
SiO_2 thermal	6	1.02×10^{-2}

For the test AR coatings, the ZrO_2/SiN x-scan shown in Figure 4a shows several spikes, with a baseline α = 57 ppm. By comparison, Figure 4b shows the ZrO_2/SiO_2 sample, which has a lower baseline α = 9 ppm, and relatively few spikes, indicating a uniform and high-quality coating. The baseline absorption measurements for all of the AR coatings are also given in Table 4.

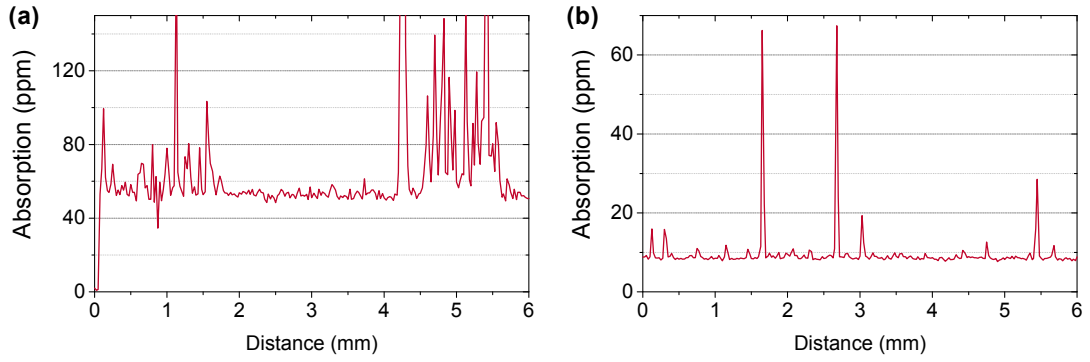

Figure 4. PCI absorption x-scan of the (**a**) ZrO_2/SiN; (**b**) ZrO_2/SiO_2 coating samples.

Table 4. PCI baseline absorption values for the AR coatings.

Coating and Deposition Technology	PCI Absorption (ppm)	PCI Absorption (ppm/nm)
//ZrO_2/SiO_2 RF sputter	9	2.76×10^{-2}
//ZrO_2/SiN DC sputter	57	1.88×10^{-1}
//Ta_2O_5/SiO_2 RF sputter	3	1.07×10^{-2}
//Ta_2O_5/SiO_2 ebeam	13	4.07×10^{-2}
//AlN/SiN DC sputter	23	7.6×10^{-2}
//AlN/SiO_2 DC sputter	6	1.58×10^{-2}
//ZnSe/LiF thermal	20	5.73×10^{-2}

4. Laser-Induced Damage Threshold and Material Properties

Laser-induced damage threshold was assessed at two facilities: Lidaris Ltd. and Quantel Inc. Lidaris used the first harmonic of pulsed Nd:YAG InnoLas Laser: SpitLight Hybrid laser (λ = 1064 nm, linear polarization, TEM00 single mode, pulse duration 9.6 ns ± 1 ns), λ/2 plate combined with additional polarizer attenuator, online scattered light damage detection, and offline inspection of damage detection using Nomarski microscopy (×100). For each sample, 411 equally spaced test sites in square grid pattern were used to reduce erratic defect-driven results and assess the threshold. The beam diameter in the target plane ($1/e^2$) was 203.6 µm. Quantel used a Q-Switched laser (λ = 1064 nm, linear polarization, TEM00 single mode, pulse duration 20 ns) with a beam diameter ($1/e^2$) of 560.0 µm, 80 test sites per sample. In accordance with the end-specification, Quantel tests were only carried out at 200-on-1.

The coating samples were tested in 1-on-1 and s-on-1 (s = 200, 1000) regimes, these are defined within the ISO 11254-1 and 11254-2 standards [4,5]. Where strong differences between each test regime exist, it is expected that the coating undergoes significant parametric change during the test, such as localized annealing and stoichiometric balancing (for example, previously unpublished internal work shows the average stoichiometry of tantalum oxide as being $Ta_{2.5}O_5$). Figures 5–7 show these LIDT results and demonstrate good agreement between these methods. The strong substrate dependence can be seen when comparing identical coatings grown on witnesses *vs.* the finished component (ZrO_2/SiO_2 in Figure 6, *qv.* Figure 7 LIDT values). In Figure 7, no failures were seen on any of the identical components below 40 J/cm^2. The PCI absorption is also plotted in Figures 5 and 6 and, for both the single-layer and AR coatings, there appears to be no direct correlation between the LIDT and coating absorption.

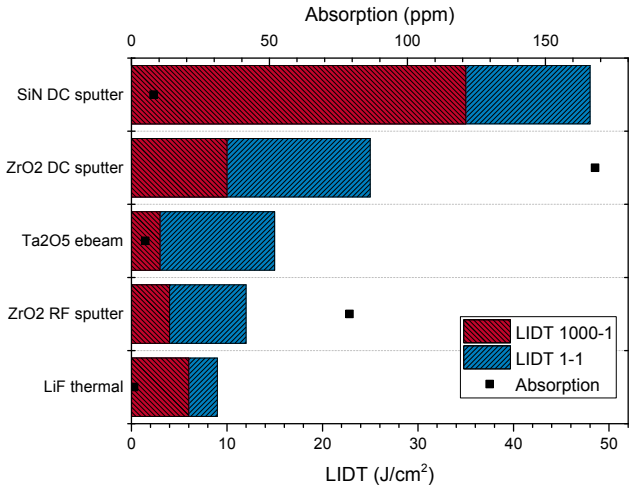

Figure 5. Comparison of 1000-on-1 and 1-on-1 the laser-induced damage threshold (LIDT) to baseline PCI absorption for the single-layer coatings.

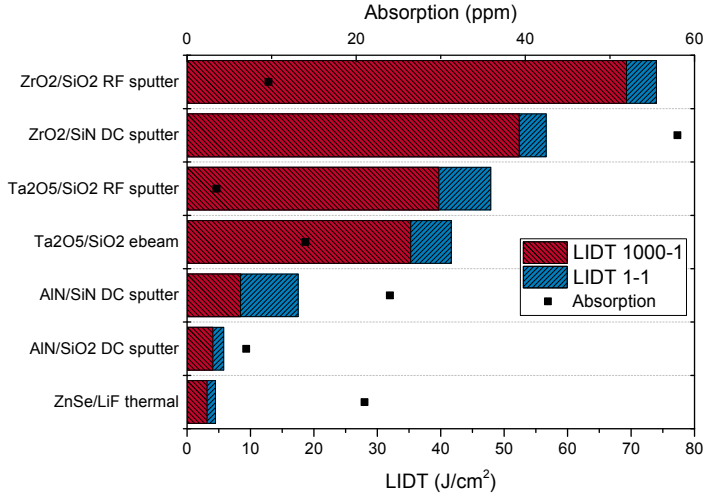

Figure 6. Comparison of Lidaris 1000-on-1 and 1-on-1 LIDT to baseline PCI absorption for the AR coatings.

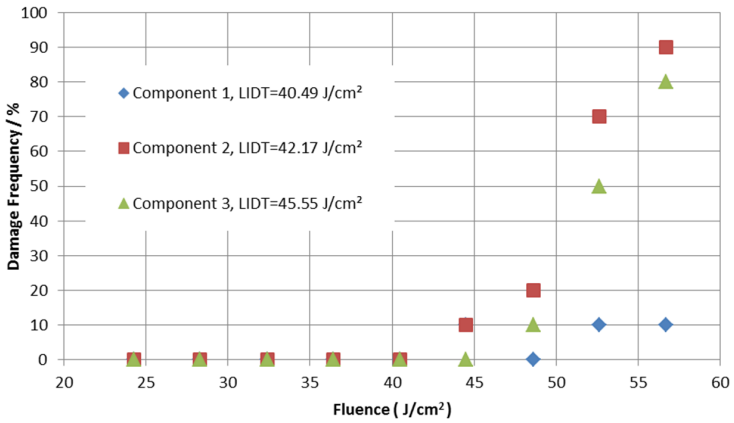

Figure 7. Quantel-tested 200-on-1 LIDT of RFS//ZrO_2/SiO_2 AR coatings on the finished components.

LIDT damage types include material-only ablation (seen in the Nb_2O_5/SiO_2 RF-sputtered coating, Figure 8a), coating loss, substrate damage (seen in the higher damage-resistant coating such as the ZrO_2/SiO_2 RF-sputtered (Figure 8b)) and substrate-only damage (seen in the case of the ZrO_2/SiN DC-sputtered coating (Figure 8c). In some ebeam coating sample cases, thermally induced local damage was also observed.

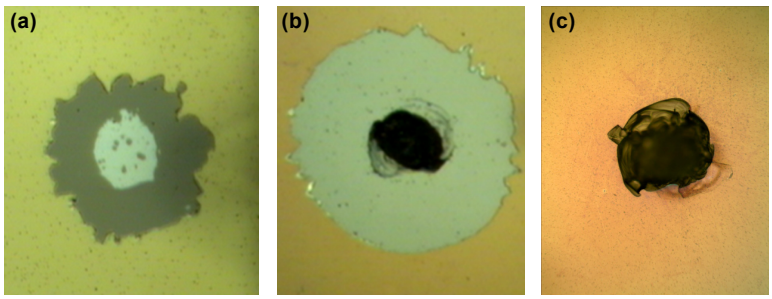

Figure 8. Optical microscope images highlighting the damage morphology of a damage pit from the (**a**) RFS//Nb_2O_5/SiO_2; (**b**) RFS//ZrO_2/SiO_2; and (**c**) DCS//ZrO_2/SiN coatings. The inner damage zone is *circa* 30 μm in diameter in each case.

AFM measurements were also made on a Veeco Dimension V AFM & Nanomechanical Tester. The AFM was set to run in contact mode with a 0.4–0.7 μm-thick non-conductive silicon nitride tip, and is typically able to measure height differences ranging from sub-nanometer to a few microns. Surface roughness, *R*, of the undamaged coating regions were also measured and gave $R = 11.1 \pm 0.6$ nm for the ZrO_2/SiO_2 coating and $R = 0.85 \pm 0.07$ nm for the Nb_2O_5/SiO_2 coating.

5. Discussion and Conclusions

The main objective of developing a coating with a LIDT greater than 20 J/cm^2 (1 GW/cm^2) was exceeded comfortably, with double this value being consistently reported. While it has been definitively shown on the final component for only one coating design, it can be demonstrated that other coating material systems have a strong potential and are likely to also meet the requirement. It was also previously reported that a post-deposition annealing at 300 °C consistently reduces absorption as measured by PCI but does not significantly increase the LIDT [6]. In the case of the ZrO_2/SiO_2 coating, the LIDT is largely limited by the substrate properties: upheld by both substrate PCI absorption measurements and the substrate failure of the top performing samples. There are many possible reasons for this lack of LIDT improvement, including that the baseline absorption is not the dominant mechanism at the measured levels-instead, e.g., electric field breakdown effects may be more prevalent. Similarly, the micro-inclusion content and nanostructure may also be critical, and this could help explain the observed improvement in RF-sputtered materials over their namesakes grown by electron beam evaporation; this can often be seen by surface roughness or by a surface PCI absorption scan.

ZrO_2 appears to have great potential (deposited by either RF or DC sputtering), offering good LIDT performance when used with either SiO_2 or SiN despite also having higher absorption in the latter case. It was expected that the nitride would have a higher damage threshold due to the higher thermal conductivity [7], which may be the case, but instead it appears limited by the substrate for these samples.

The surface variability in absorption offers deposition technique-related clues that point to the need for higher chamber cleanliness and better control of inclusions (longer source conditioning, better source cleaning, lower deposition rates, longer source-to-substrate separation, *etc.*), and may also require better substrate cleaning and handling.

From the range of PCI absorption measurements collected for the uncoated substrates (a factor of 400 for seemingly identical transmission by spectrophotometry), an observed enhancement of scratches after laser damage testing on some samples, and an apparent threshold ceiling prior to substrate failure, it would seem prudent to ensure a more standardized starting point for future substrate selection based not only on internal losses but also surface finish, for which such a correlation has long been reported [8]. Future work would therefore include before-and-after laser damage microscale surface analysis.

It is clear that in some cases the absorption appears to be reduced by the addition of an additional layer. The mechanism is not known but could be due to the prolonged exposure to oxygen plasma, for example, during the second layer or an induced transmission effect or simply variation in the deposition process. Further work is planned to investigate this.

Further investigations planned will explore alternative high index materials including HfO_2 and different starting materials for the same final coating chemistry for the reactive ebeam, such as Nb_2O_5 from Nb metal and SiO_2 from Si, to reduce inclusions and scatter centers. It would also be interesting to complete the analysis on single layers such as AlN and ZnSe. A study of the effect of the sputtering rate of ZrO_2 on the intrinsic properties and any resultant change in LIDT would also be desirable, given the demonstrated promising performance of the material.

Acknowledgments: The authors would like to thank the SU2P (www.su2p.com) for funding through the Pilot Project scheme, and in particular Iain Ross who was instrumental in the facilitation of this collaboration.

Author Contributions: Caspar Clark designed and fabricated the optical coatings and oversaw Lidaris LIDT tests; Riccardo Bassiri and Ashot Markosyan performed PCI measurements and analysis; Martin M. Fejer provided experimental expertise to PCI analysis; Des Gibson oversaw and analyzed Quantel LIDT tests; Iain W. Martin, Peter G. Murray, Joseph Tessmer and Sheila Rowan performed AFM, ellipsometry, and photostructural analysis; Caspar Clark, Riccardo Bassiri and Iain W. Martin were the lead investigators and responsible for securing the SU2P Pilot Project funding for this research.

Conflicts of Interest: The authors declare no conflict of interest.

References

1. Furukawa, Y.; Kitamura, K.; Alexandrovski, A.; Route, R.K.; Fejer, M.M.; Foulon, G. Green-induced infrared absorption in MgO doped $LiNbO_3$. *Appl. Phys. Lett.* **2001**, *78*, 1970–1972. [CrossRef]
2. Alexandrovski, A.; Fejer, M.; Markosyan, A.; Route, R. Photothermal common-path interferometry (PCI): New developments. In Proceedings of the SPIE, the International Society for Optical Engineering, San Jose, CA, USA, 24 January 2009.
3. Markosyan, A.S.; Route, R.; Fejer, M.M.; Patel, D.; Menoni, C.S. Spontaneous and induced absorption in amorphous Ta_2O_5 dielectric thin films. In Proceedings of the Annual Symposium on Optical Materials for High Power Lasers, Boulder, CO, USA, 18 September 2011.
4. *ISO 11254-1:2000 Lasers and Laser-related Equipment—Determination of Laser-induced Damage Threshold of Optical Surfaces—Part 1: 1-on-1 Test*; ISO: Geneva, Switzerland, 2000.
5. *ISO 11254-2:2001 Lasers and Laser-related Equipment—Determination of Laser-induced Damage Threshold of Optical Surfaces—Part 2: S-on-1 Test*; ISO: Geneva, Switzerland, 2001.
6. Bassiri, R.; Clark, C.; Martin, L.W.; Markosyan, A.; Murray, P.G.; Tessmer, J.; Rowan, S.; Fejer, M.M. Investigating the relationship between material properties and laser-induced damage threshold of dielectric optical coatings at 1064 nm. In Proceedings of the SPIE, Laser-Induced Damage in Optical Materials, Boulder, CO, USA, 23 November 2015.
7. Guenther, A.H.; McIver, J.K. The role of thermal conductivity in the pulsed laser damage sensitivity of optical thin films. *Thin Solid Films* **1988**, *163*, 203–214. [CrossRef]
8. House, R.A.; Bettis, J.R.; Guenther, A.H. Correlation of laser-induced damage threshold with surface structure and preparation techniques of several optical glasses at 1.06 μm. *NBS Special Publ.* **1975**, *435*, 305–320.